PR12-18-006

Search for New Physics in e^+e^- Final States Near an Invariant Mass of 17 MeV Using the CEBAF Injector

The DarkLight Collaboration

R. Alarcon, G. Randall

Arizona State University, Tempe, AZ

T. Cao, B. Dongwi, I. P. Fernando, P. Guèye, M. Kohl,

A. Liyanage, J. Nazeer, T. Patel, M. Rathnayake

Hampton University, Hampton, VA

J. Grames, R. Kazimi, M. Poelker, S. Benson, J. Boyce, J. Coleman, D. Douglas,

S. Frierson, C. Hernandez-Garcia, M. McCaughan, C. Tennant, S. Zhang

Thomas Jefferson National Accelerator Facility, Newport News, VA

J. Bessuille, P. Fisher, I. Friščić, D. Hasell,

E. Ihloff, R. Johnston, J. Kelsey, S. Lee, P. Moran,

R. Milner, C. Tschalär, C. Vidal, Y. Wang

Laboratory for Nuclear Science, MIT, Cambridge, MA

J. C. Bernauer, E. Cline, R. Corliss, K. Dehmelt, A. Deshpande

Stony Brook University, Stony Brook, NY

Co-Spokespeople: Jan Bernauer[a], Ross Corliss, Peter Fisher, and Richard Milner

(Dated: December 29, 2019)

[a]jan.bernauer@stonybrook.edu

Abstract

In a revised version of Jefferson Laboratory Proposal PR12-18-006, the DarkLight collaboration proposes a run of 1000 hours (45 days) at the CEBAF injector (45 MeV beam with 150 µA current) to search in the e^+e^- invariant mass region around 17 MeV in electron scattering from tantalum for evidence of new physics, motivated by anomalies resulting from the muon $g-2$ determination and reported in the decays of excited ^{8}Be and ^{4}He. By covering all remaining possible coupling range, it will be the definitive experiment to test for the existence of a dark fifth-force carrier, proposed to explain the ^{8}Be anomaly. If scientifically approved and funding is immediately available, the experiment can begin data taking in 2020. The experiment can form the basis for M.S. and Ph.D. theses for graduate students at Arizona State University, Hampton University, MIT and Stony Brook University.

I. SCIENTIFIC OVERVIEW

The search for an understanding of the elusive Dark Matter is one of the great scientific quests of our age. In the 1930s, astronomers first made determinations of the gravitational mass of galaxies that were significantly larger than expected from the observed luminosities and wrote of *dunkle Materie* [1]. Almost ninety years later, there is collective evidence that is substantial and consistent across seven orders of magnitude in distance scale (from about 1 kpc to 10 Gpc) that an unknown substance—dark matter—shapes the large-scale structure of the universe.

We can infer a great deal from the gravitational effects of dark matter: We know the approximate density and velocity of dark matter in our galaxy, and that it does not form tightly bound systems larger than about 1,000 solar masses. It is also abundant, seeming to account for about 25% of the mass of the universe, about five times larger than the matter we can see. In our current understanding, the known, uncharged particles, i.e. the neutron or neutrino, cannot be a major component of the inferred dark matter mass, and so we posit at least one as-yet unobserved new particle.

This particle must obviously interact gravitationally, but we expect it also interacts with the visible universe through other mechanisms, with coupling on the order of the weak interaction or less, in order for dark matter to be in equilibrium with other matter in the early universe.

The focus over several decades has been to look for a particular type of possible dark matter, a Weakly Interacting Massive Particle (WIMP), via a rare scattering from an atom in a large detector, typically located deep underground to minimize the rate of background events. The WIMP mass region explored by such experiments typically ranges from about 3 GeV to 10 TeV, and present experiments have probed WIMP-atom interaction cross sections lower than about 10^{-46} cm^2 at a WIMP mass of about 50 GeV. Thus far, no conclusive evidence for WIMPs has been found. Searches for WIMPs will continue for at least another decade. However, there is a fundamental floor on this approach due to the inability to distinguish between a neutrino-atom interaction and a WIMP-atom interaction.

A complementary experimental thrust in the quest to understand dark matter is to search for evidence of the mediator of a new interaction between our visible world, successfully described in terms of four forces (gravity, electricity and magnetism, nuclear force and weak

force), and the world of dark matter. This new interaction would constitute a fifth force. The simplest mediator widely considered is a dark photon, A', that couples to the known particles via their electric charges. The searches involve experiments using particle beams delivered by accelerators to produce the mediator. This mediator decays either into (a) known, detectable particles that are sought (*visible decays*) or (b) into dark-sector particles, which are undetectable, but whose presence is deduced by observation of a large missing energy and momentum in the final-state (*invisible decays*). The results of the searches are usually summarized in terms of their ability to constrain the mediator-to-known-matter coupling strength and the mediator mass. At the Large Hadron Collider at CERN, Geneva, Switzerland, searching for evidence of dark matter is a major activity at the collider experiments.

Recently, there has been a focus on a mediator with mass lower than 1 GeV. Astrophysical observations, and observed anomalies in measurements involving the muon and nuclear transitions, hint at this possibility. There have been extensive searches for the dark photon, mainly in existing experiments π^0-decay and much of the parameter space of coupling and mass that corresponds to these anomalies is excluded at 2σ. However, a more general fifth force, where the couplings are no longer directly proportional to the electric charges, can not yet be ruled out.

It is straightforward to adjust the quark couplings of a fifth force to satisfy existing constraints and still allow such a force acting via lepton coupling can produce a signal. A number of recently-reported anomalies motivate further searches for such an effect at low energies. Studies of decays of an excited state of ^{8}Be to its ground state have found a 6.8σ anomaly in the opening angle and invariant mass distribution of e^+e^- pairs produced in these transitions [12], and a similar anomaly has recently been announced in ^{4}He[13]. While these discrepancies may be the result of as-yet-unidentified nuclear reactions or experimental effects, they can be explained by the production of a new boson with a mass around 17 MeV. In addition, although the effect may yet be reconciled within the context of the Standard Model, the observed 3.5σ deviation between the measured and expected anomalous magnetic moment of the muon can also be explained by such a fifth force with mass in the range 10 to 100 MeV.

II. THE DARKLIGHT EXPERIMENT

Motivated by these considerations, the DarkLight (Detecting A Resonance Kinematically with Leptons Incident on a Gaseous Hydrogen Target) experiment was conceived at MIT-LNS in 2008, initially as a search for a dark photon, A', using elastic electron-proton scattering at an incident electron beam energy of 100 MeV. Operating below pion threshold, where the final-state is simplest, the experiment would be sensitive to the decay of this new boson to e^+e^- (*visible*) or to a dark sector fermion−antifermion pair, $f\bar{f}$ (*invisible*). The methodology employed here is well established as a means to search and discover new physics, *e.g.* the discovery of the J/ψ [5], and has been employed successfully recently at Jefferson Laboratory [6].

A detailed proposal developed by the DarkLight collaboration was submitted to the Jefferson Laboratory Program Advisory Committee (PAC), reviewed, and fully approved with "A" scientific rating in May 2013. This was motivated by the unique Energy Recovery Linac (ERL) at the Free Electron Laser, now called the Low Energy Recirculator Facility (LERF). A run in July 2012, in which technical feasibility was demonstrated [2], was key to establishing full approval. Within a year, a phase-1 DarkLight experiment based on an existing 0.5 Tesla solenoidal magnet was funded by the NSF through its MRI program with three scientific goals:

- **Phase-1a** Install the existing solenoidal magnet and the gas target to operate up to full thickness. In addition, install detectors to measure rates and to gain valuable experience in understanding detector performance. The principal goal was to study how the magnet and target affect the characteristics of the 100 MeV ERL beam as a function of solenoidal magnetic field strength, target thickness, and ERL beam current.
- **Phase-1b** Measure radiative Møller scattering at 100 MeV using a thin carbon foil target. This is an important background for the full physics measurement, and has been calculated by our collaboration. Its measurement requires a distinct detector configuration involving a magnetic spectrometer to detect the 1 to 5 MeV final-state electrons at angles from 25° to 45°.
- **Phase-1c** Carry out a preliminary search for a bump in the e^+e^- final-state.

In summer 2016, the phase-1 DarkLight experiment was installed at the Jefferson Laboratory

TABLE I: Chronology of major milestones of the DarkLight experiment in the years 2010-2019.

Date	Milestone
Jan 2010	Letter of Intent submitted to Jefferson Laboratory PAC35: encouraged to develop a full proposal
June 2012	DarkLight proposal C12-11-008 submitted to PAC39: approved for 90 days at LERF: "A" scientific rating and C1 technical condition
July 2012	Successful, stable transmission of 0.5 MW ERL beam through a narrow aperture with low background [2, 4, 7] satisfying the condition
Nov 2012-Mar 2013	Technical review of DarkLight by *ad hoc* Jefferson Lab committee
May 2013	Full scientific approval with "A" rating by JLab Director
Jan 2014	Submission of proposal to NSF MRI solicitation for a phase-1 DarkLight experiment led by MIT
July 2014	MRI Award by NSF to: ASU, Hampton U., MIT, and Temple U.
Aug 2014-Jul 2016	Design & construction of phase-1 DarkLight experiment
Dec 2015	Readiness review
Jul-Sep 2016	Installation and initial commissioning of phase-1 DarkLight at LERF
2017	Jefferson Lab repurposes LERF for LCLS cavity testing
2017 - 2018	Measurement of low-energy Møller scattering carried out at MIT
2018	Concept for 17 MeV search at CEBAF injector developed
July 2018	Proposal PR12-18-006 submitted and deferred by PAC46
December 2019	Proposal PR12-18-006 revised with new scientific motivation

LERF and initial commissioning took place [3]. In 2017, the LERF was repurposed as a cavity testing facility for LCLS cavities and no further LERF running for physics experiments is planned for the foreseeable future.

Accordingly, we have carried out a measurement of low-energy Møller scattering at 2.5 MeV using the Van de Graaff accelerator at the MIT High Voltage Research Laboratory to address the scientific goal of 1b. This project, summarized in the Appendix, was completed in fall 2018.

The principal focus of the DarkLight Collaboration for the next several years is the search for new physics in e^+-e^- final states around 17 MeV invariant mass, motivated by the recent ^{8}Be anomaly. We believe that this proposed experiment, at the CEBAF injector, is the best possible approach to address this important scientific goal.

Table I summarizes the chronology of major milestones in the years 2010-2019.

We note that interest in the DarkLight experiment has remained high with recent articles in *Nature* [8], *The Washington Post* [9], *Research Features* [10] and *Open Access Government* [11].

III. MOTIVATION FOR PROPOSED CEBAF INJECTOR EXPERIMENT

In 2016, a Hungarian group reported [12] an anomaly in the invariant mass and angular distribution spectra of e^+e^- pairs from ^{8}Be* decay which could be interpreted as evidence of a new light neutral boson with mass around 17 MeV, as shown in Fig. 1(a). Nuclear physics calculations of this decay process do not eliminate the anomaly [15]. Further, it has been realized [16] that by tuning the couplings all existing exclusion limits for dark photons may be satisfied and the ^{8}Be anomaly may be explained. Recently, the Hungarian group has reported [13] additional evidence for a mass around 17 MeV in measurements of electron-positron pairs from the electromagnetically forbidden M0 transition from the 21 MeV state in ^{4}He, as shown in Fig. 1(b). These results have attracted great attention in the popular media [14], and urgently demand independent experimental verification.

Motivated by these developments, we have reconsidered the design of our experiment PR12-18-006 to use the 45 MeV electron beam from the CEBAF injector as presently configured to search for the reported anomaly in e^+e^- final-states in scattering from a tantalum target.

A. Fifth Force Parameter Space

The existing exclusions on the production of dark photons can be divided into measurements observing hadronic production mechanisms (e.g. π^0 decay) and those observing leptonic production mechanisms (e.g. e-p scattering, e^+e^- annihilation). In the simplest dark photon model, the effective coupling to a new force-carrier is proportional to electric charge,

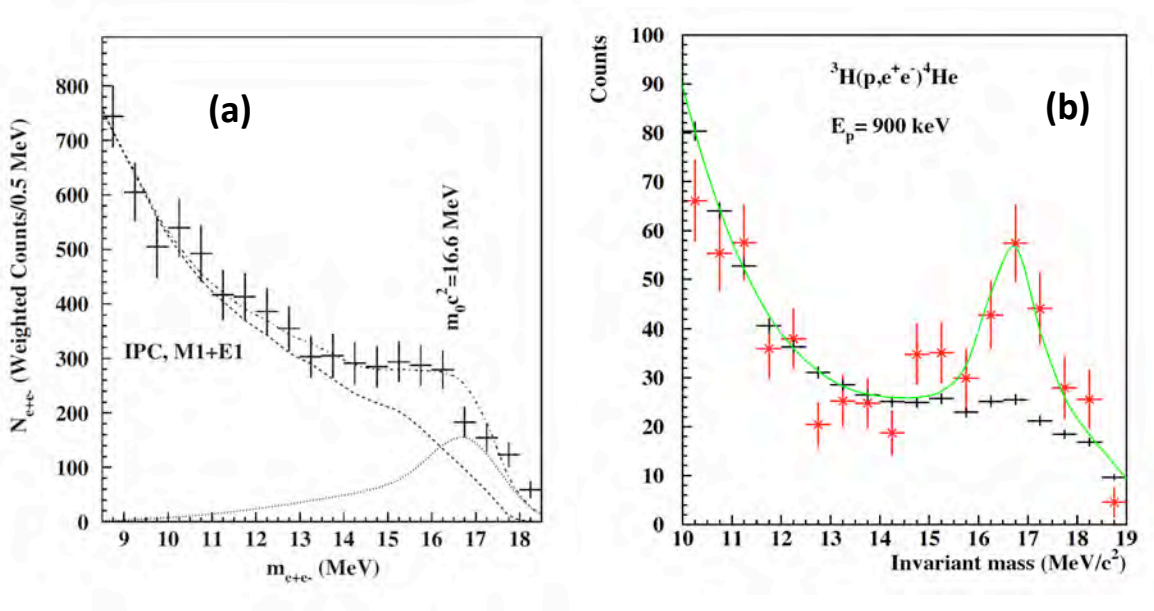

FIG. 1: (a): Anomaly on ^{8}Be [12]. (b): Anomaly on ^{4}He [13].

so all these exclusions apply to the same parameter space, but in more generic fifth-force models [16] this restriction is relaxed.

The wider parameter space has multiple couplings—most generally an independent coupling to each flavor of quark or lepton. Since these couplings are no longer directly linked, many of the experiments which probe the ^{8}Be anomaly region in the simplest dark photon model, and which depend on various hadronic couplings, no longer directly inform the coupling to electrons. Indeed, the $g-2$ and ^{8}Be anomalies suggest a particle whose coupling to some quark flavors is significantly suppressed, implying a substantially reduced sensitivity in some hadronic production modes.

The strongest remaining constraints on the electronic coupling near the ^{8}Be anomaly region come from measurements by NA64[17] for small couplings, and from electron g-2 measurements for large couplings, with a key region of the anomaly region still untested (see Fig. 2). New results of NA64, available as a preprint [18], will include a larger statistical sample and will push the lower exclusion bound at the relevant mass up to $\epsilon^2 \approx 5 \times 10^{-7}$. First calculations indicate that the effect found in ^{4}He would be compatible with a similar coupling range.

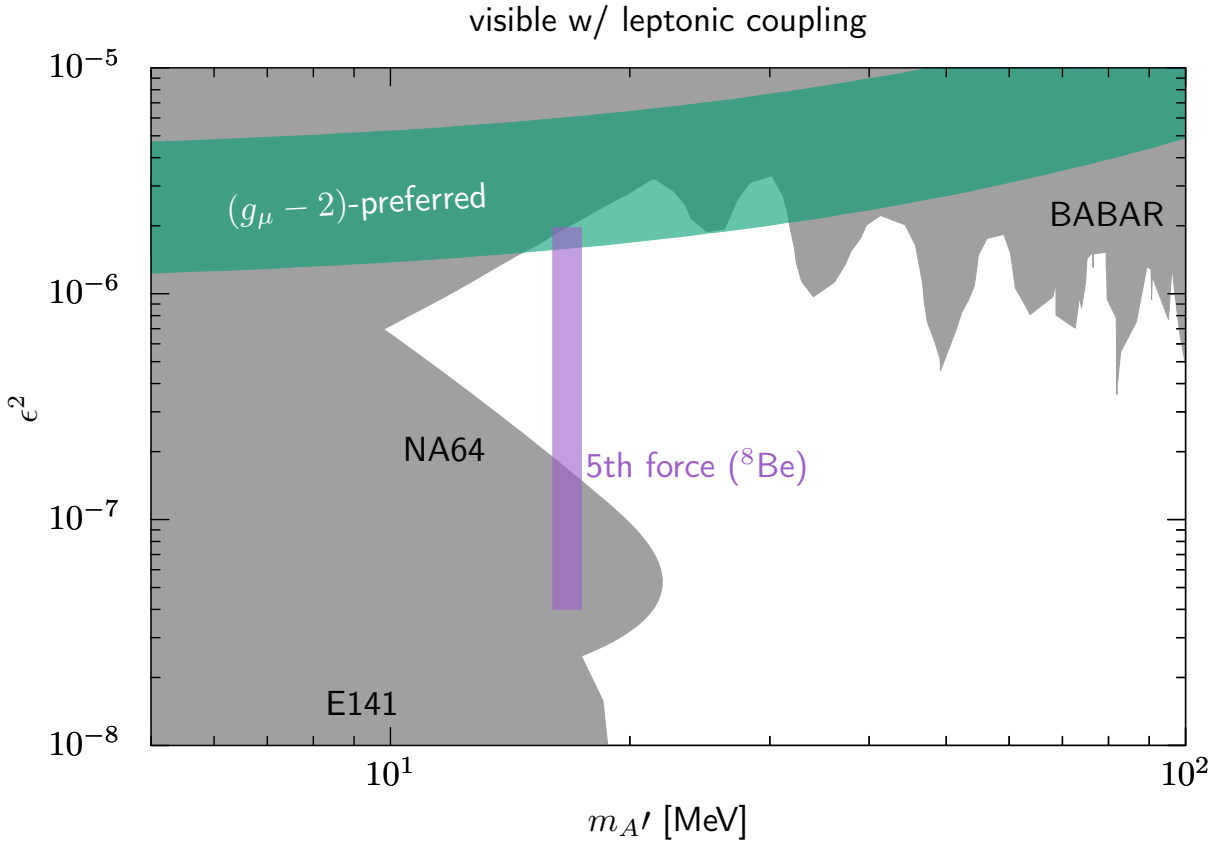

FIG. 2: Parameter space for a fifth force, with ^{8}Be and $g-2$ anomalies in color. Vertical axis is the leptonic coupling strength. Excluded regions, in gray, are taken from experiments that have no dependence on hadronic couplings.

A program to fully search the available parameter space for corroboration of the ^{8}Be anomaly will require both leptonic and hadronic probes: If a new particle is observed in one of these modes, it will be of utmost interest to measure all of its couplings. If it is not observed, both modes will be needed in order to definitively rule out the couplings required for the production of the new boson inside the beryllium nucleus and its prompt decay into

electrons.

The LHCb collaboration has proposed an inclusive search for a dark photon in electron-positron pairs in LHC Run 3 (planned to complete data-taking in 2022) with sensitivity to a large region of the original A' parameter space. They also collected a smaller dataset in 2018 which contains tagged η and π^0 events with electron-positron pairs.

Purely leptonic searches that can be undertaken on similar time scales, like the one proposed here, will form the leptonic counterpart to hadronic experiments like LHCb, and clarify the interpretation of the latter's results by narrowing the range of allowed electron coupling.

B. Kinematics at the CEBAF Injector

In the original concept for the LERF-based experiment, sensitivity at the low-mass dark photon region is limited by the kinematics of the production mechanism, with the majority of the dark photons boosted significantly forward and decaying into leptons falling below the minimum transverse momentum for the tracking detectors. The use of the CEBAF injector has the benefit of allowing a lower beam energy than in the original design, reducing the boost of a dark photon and opening up the small angles of these forward-going decay leptons.

The experiment proposed here takes advantage of these larger angles. We propose a two spectrometer setup optimized for the anomaly region and using a thin foil target to achieve sufficient luminosities. The details of this approach are presented in the next section.

IV. EXPERIMENT DESIGN

The proposed experiment aims to measure the process $e^- X \to e^- Ta A' \to e^- Ta(e^+e^-)$ as a resonant excess of e^+e^- pairs at the invariant mass of the A'. The produced leptons are detected by a pair of dipole spectrometers arranged asymmetrically around a fixed foil target placed in the 45 MeV beamline available at the CEBAF injector.

A. The CEBAF Injector

1. Beam Parameters

The CEBAF photoinjector includes three spectrometer beamlines used to set the beam energy at different acceleration stages. Besides serving this diagnostic function, spectrometer beamlines have also been used to conduct dedicated R&D. This experiment would be located on the 4D spectrometer beamline (Fig 3). During normal 2 K operations, the beam energy delivered to that point can be varied from 17 to 125 MeV, and can be measured with 0.1% precision. The beam energy spread is of the order 0.1% and the rms electron bunch length approximately 0.5 ps. The transverse design emittance is 3×10^{-9} meter-rad leading to rms transverse beam size of 100-200 μm.

The CEBAF injector drive lasers typically generate beams with 249.5 or 499 MHz bunch repetition rates, but can be configured to provide 1497 MHz repetition rate for a single user. At this bunch repetition rate, one drive laser can provide ~ 200 μA to the 4D spectrometer line with high transmission through upstream injector apertures, and with long operational lifetime (weeks of uninterrupted beam delivery).

Spin polarized electron beams are typically produced at the photoinjector, but unpolarized beam can be delivered by de-energizing the drive laser Pockels cell.

A short period for developmental beam studies will be needed to configure the injector for beam delivery using a single laser 1497 MHz mode and to converge on appropriate lattice optics for the desired spot size. We estimate the scope of work would last approximately three days, with two days dedicated to laser reconfiguration and injector setup and the final day devoted to studies of the beam optics.

We have considered the optimal energy for the experiment and find it to be 45 MeV. Somewhat lower energy will reduce the optimal figure of the experiment somewhat and the

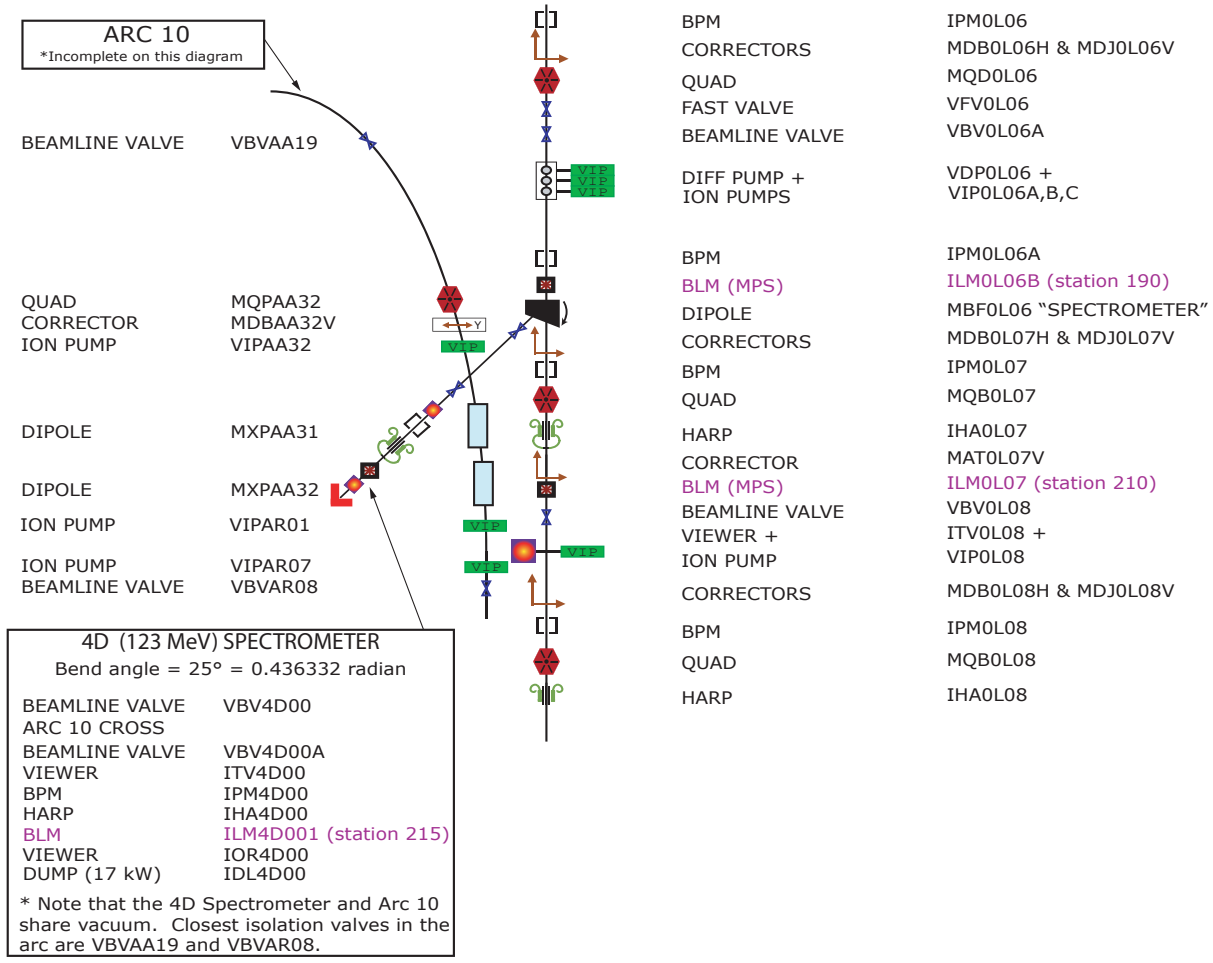

FIG. 3: The CEBAF injector layout in the vicinity of the proposed experiment. Beamline elements are at their approximate positions, but distances and sizes are not to scale. Further injector beamline elements upstream of the upper beam position monitor (IPM0L06) and downstream of the HARP (IHA0L08) are not shown. The injector beam can be diverted by the dipole (MBFOLO6) into the 4D Spectrometer region, in which the target and spectrometers would be placed.

incident energy must obviously be significantly higher than 17 MeV.

2. 4K Operation

Recent demonstrations indicate beam delivery to the 4D injector beamline is possible when SRF accelerating cavities are at 4 K, which is a typical condition during scheduled accelerator shutdowns. The maximum beam energy at the 4D line under this condition,

sustained reliably, is of the order of 20 MeV, which is of interest for commissioning of the experiment.

B. Target

The experiment design assumes a 45 MeV e^- beam provided by the CEBAF injector with a current of 150 µA. It will impinge on a 10 µm tantalum foil. This produces an instantaneous luminosity of $\mathcal{L} = 52\,\mathrm{nb}^{-1}\,\mathrm{s}^{-1}$, i.e., $0.275\,\mathrm{fb}^{-1}\,\mathrm{s}^{-1}$ hydrogen equivalent, and will cause a beam spread of approximately 0.5° downstream of the target.

The beam will heat up the foil with about 4 W, which can be dissipated via radiation for practical beam spot sizes. To protect the target from accidental melting, the target will be a spinning foil disc. This will be Fast Shutdown (FSD) interlocked to protect the accelerator in the event the disc stops spinning.

C. Beam Dump

The 0L07 beam dump at the end of this line can dissipate 17 kW of beam power. The maximum current delivered to the dump can be calculated using the standard relationship $P = IV$, where V is the beam energy. At 50 MeV, the 0L07 dump can take beam currents of up to 340 μA. At the proposed settings, the beam will deposit less than 8 kW into the dump, well within this envelope.

D. Spectrometer

The experiment will make use of two dipole spectrometers, with very similar magnetic characteristics, under design and to be built by MIT. The spectrometer design is similar to that of the spectrometer previously constructed for the radiative Møller scattering measurement and currently in use at MIT (see Appendix). For each spectrometer, the solid angle acceptance is 12 msr, and the momentum acceptance is ±20%. A full list of design parameters is presented in Table II.

An initial conceptual design of the spectrometers has been completed, demonstrating that the desired features are readily achievable. Further optimization will be carried out

TABLE II: Design parameters for the spectrometers.

	Spectrometer	
Parameter	e^+	e^-
In-plane acceptance	$\pm 2^\circ$	
Out-of-plane acceptance	$\pm 5^\circ$	
Momentum acceptance	$\pm 20\,\%$	
Central angle	16°	33.5°
Central momentum	28 MeV	15 MeV
Dipole field	0.32 T	0.164 T
Nominal bend radius	30 cm	
Pole gap	4 cm	

and a full simulation of the field will be produced once finalized.

The two spectrometers will be operated at different currents to produce the desired magnetic fields, but share a common magnet design. They are conventional iron-core magnets with simple, planar coils. The focusing design of the magnet was optimized for 0.5 m distance from target to spectrometer entrance and pole face rotations to project particles to allow the use of three layers of 40 cm GEM tracking. The final engineering of the magnet will include detailed design optimization to increase magnetic performance, minimize size, and maximize clearance to the exit beamline. The magnet in its present configuration weighs about 950 kg. The magnets will have full fiducialization to allow for laser tracking alignment and a six-strut mechanical support system to allow for 200 micron alignment (similar to other MIT-Bates designs). The magnets will be magnetically mapped at JLab prior to installation. The electrical needs of the spectrometer are modest, 20 A at 40 V (under a kilowatt). Air cooling is used in the present configuration.

Figure 4 is an overhead view of the beamline with a possible placement of the target chamber and spectrometers.

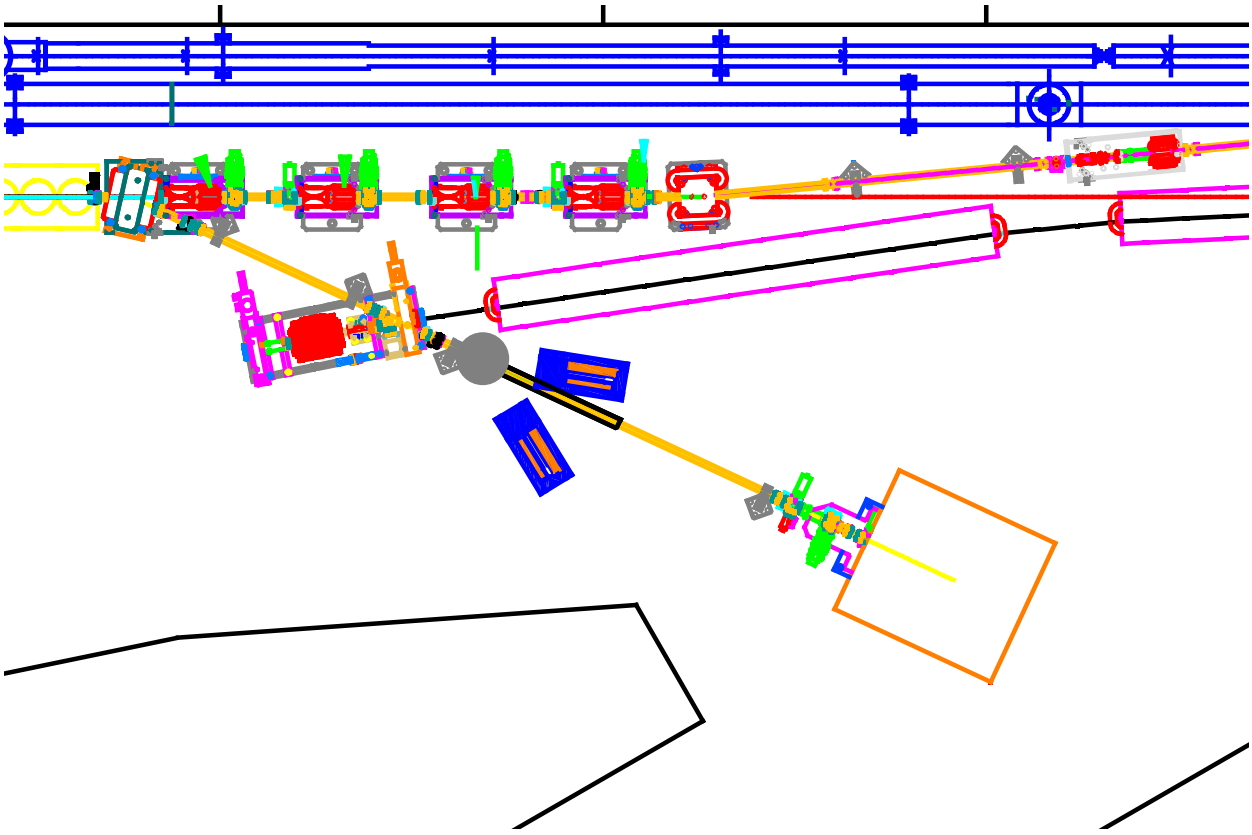

FIG. 4: Overhead view of the relevant beam line segment including spectrometer magnets, target chamber and beam dump. Drawn is a positioning most upstream, to maximize space between wall and spectrometer and distance to beam dump. A shift to a more downstream position is possible if the upstream clearance needs to be increased. (Note: The magnet yoke overhangs the beam pipe and creates an apparent interference in this projection which is not real.)

E. Detectors

Each spectrometer will be instrumented with a focal plane detector consisting of three GEM detector planes, read out via standard APV electronics. They will be provided by the Hampton University group. A segmented trigger detector, made from scintillating paddles with PMT readout, will be constructed by MIT and Stony Brook. Figure 5 depicts a schematic layout of the spectrometer and detector package.

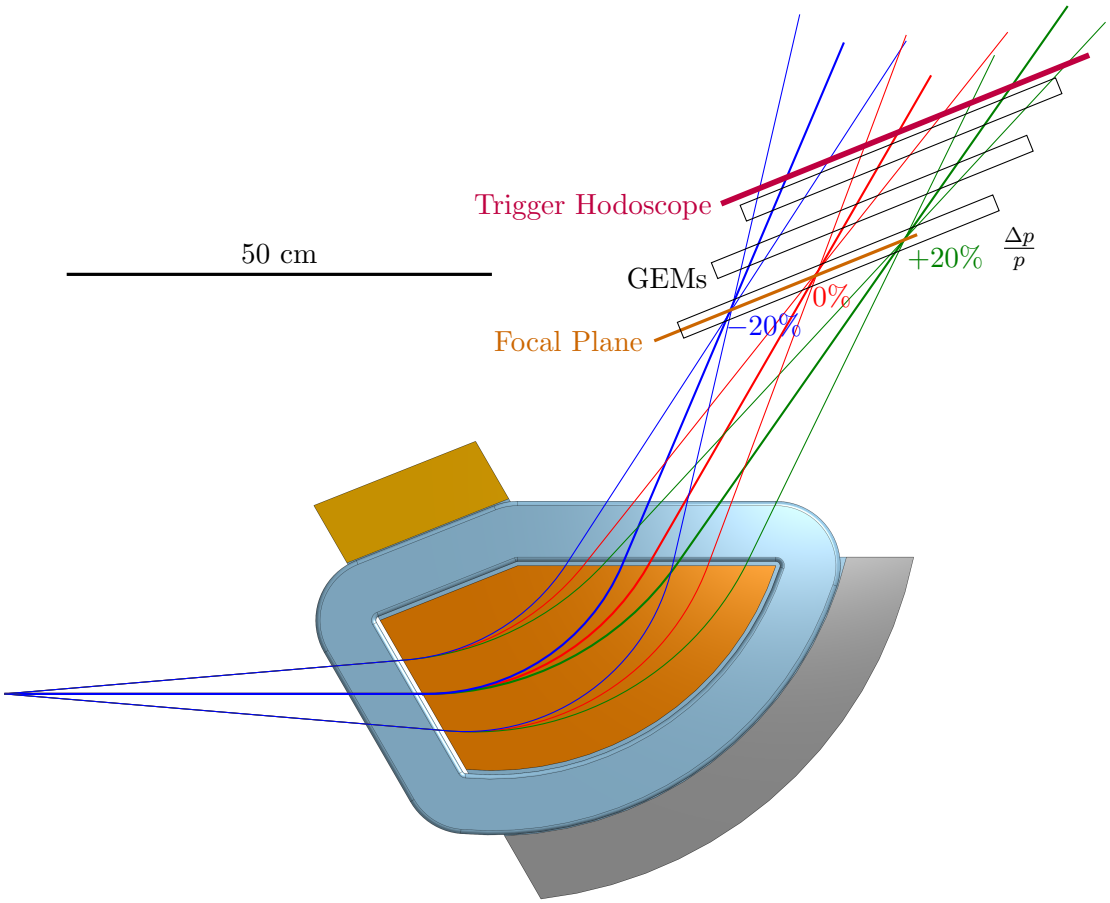

FIG. 5: Schematic overview of the spectrometer optics and detector package. Red is the central momentum p_0, with blue and green corresponding to $p_0 - 20\%$ and $p_0 + 20\%$, respectively.

1. Trigger Hodoscopes

The standard GEM readout requires a trigger signal, to be generated from the coincidence of two fast trigger detectors in the spectrometers. To reduce accidental coincidences in the trigger logic, it is important to resolve the beam bunch clock of 1497 MHz, at least on the analysis level. This timing information must be provided by the trigger detector, but can be corrected by the particle path length reconstructed from the tracking detector information. However, to reduce readout dead-time, it is important to be close to the ideal timing during data-taking. The main time dispersion is generated by the momentum-dependent dispersion inside the spectrometers. We therefore propose a trigger detector made from scintillator paddles, divided along the dispersive direction into 10 segments, each read out via a photo-

multiplier tube. These segments can then be timed in individually. The large signal from the PMTs (compared to SiPMs) and a constant fraction discriminator then allows for small coincidence time windows.

The scintillator paddles will be made from a standard plastic scintillator material, and have a size of about 150x30x2 mm^3.

2. GEM detectors

Each spectrometer will be instrumented with an identical tracking detector system consisting of three triple-GEM elements. Eight such GEMs have been designed and built with funding from the NSF MRI award and are being commissioned as of December 2019.

With an active area of 25x40 cm^2 the GEM detectors cover ten times more area than the 10x10 cm^2 GEMs used in the 2016 prototype detector[1]. The intermediate size makes the envisioned set of GEM chambers also attractive for further use in other setups.

The GEM chambers have been built as triple-GEM detectors with a standard two-dimensional readout structure with 400 μm pitch between strips. The front-end electronics are based on APV front-end cards and Multi-Purpose Digitizers (MPD) of the latest generation (APV4.1 and MPD4.0), very similar to the system used previously at OLYMPUS and DarkLight Phase-1a, and presently at MUSE. A system of GEMs+APVs+MPDs has recently been mass-produced at a larger scale for the Super-Bigbite Spectrometer (SBS) construction at Jefferson Lab.

Single-mask technique

The need to routinely construct large-area GEM detectors with reproducible gain has been met by adopting the single-mask technique to produce GEM foils. Previously, the size of GEM foils with the standard double-mask technique had been limited due to accumulative misalignment of the two opposing photo masks. Problems resulted in the non-central regions where the hole geometry was increasingly deformed, resulting in gain non-uniformity and inefficiency.

[1]Originally built by the Hampton group for the OLYMPUS experiment through an NSF/MRI award, these detectors were used in the DarkLight Phase 1a commissioning at the LERF and are also in use at MUSE.

With the single-mask technique, a hole alignment is no longer required, and largely uniform gains have been achieved. Figure 6 shows a comparison of the two schemes. The key step has been the electro-etching of the bottom copper layer with galvanic protection of the top layer. The CERN workshop is now able to routinely produce high-quality GEM foils of up to 2 m in length. The maximum size is only limited by the machines hosting the chemical etching bath.

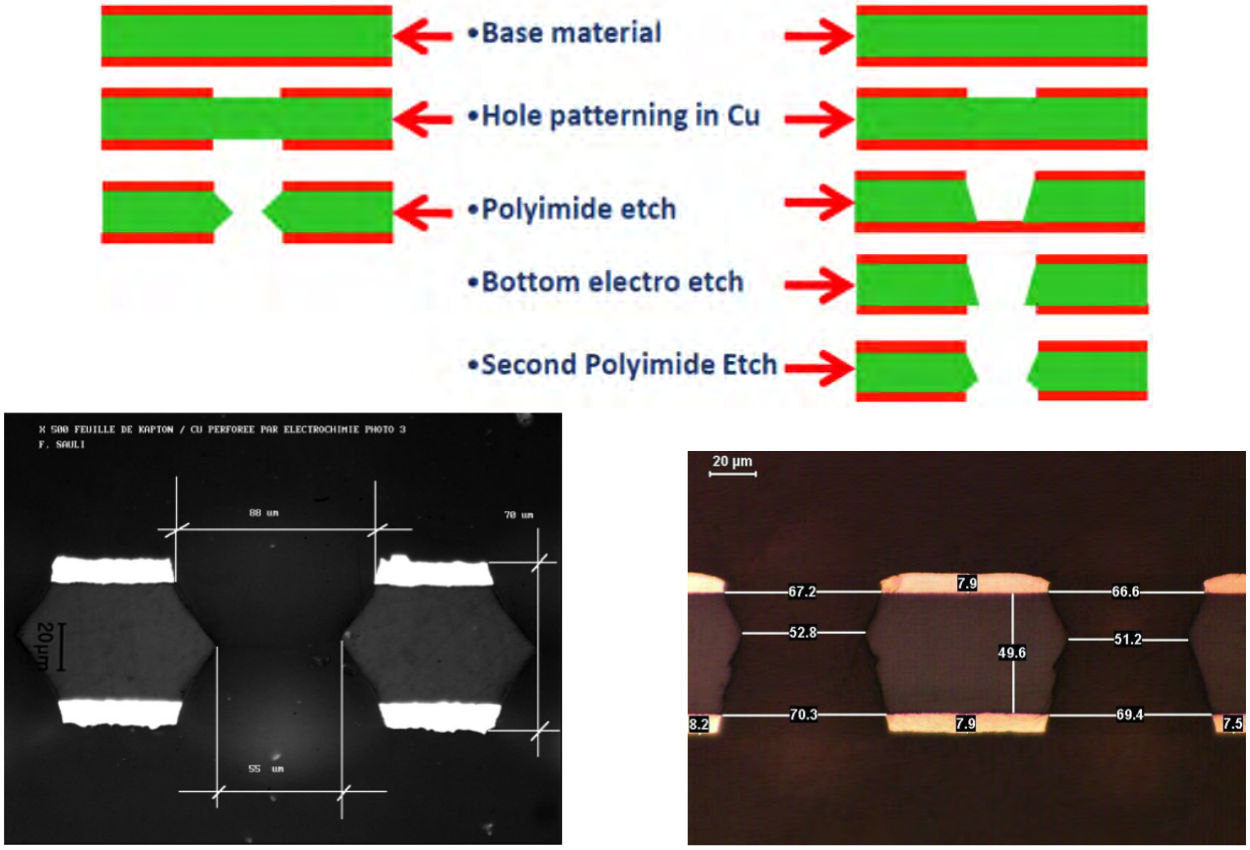

FIG. 6: Left: Double-mask etching technique. Right: Single-mask technique.

NS2 Concept

A novel technique called NS2 ("No Stretch-No Stress") has been adopted to assemble the detectors. This consists of a mechanical system to stretch the foils, which avoids the conventional gluing of the foils to frames and allows the foils to be stretched with greater tension than with the foil-on-frame gluing technique. Subsequently, no spacer grid is required, eliminating dead areas and improving the gas flow inside the chamber. This design

has been developed at CERN in the context of the CMS upgrade at LHC. For that project, a large number of large-area GEM detectors in trapezoidal geometry, ~ 1.5 m long elements for the forward muon endcap have been under construction at CERN.

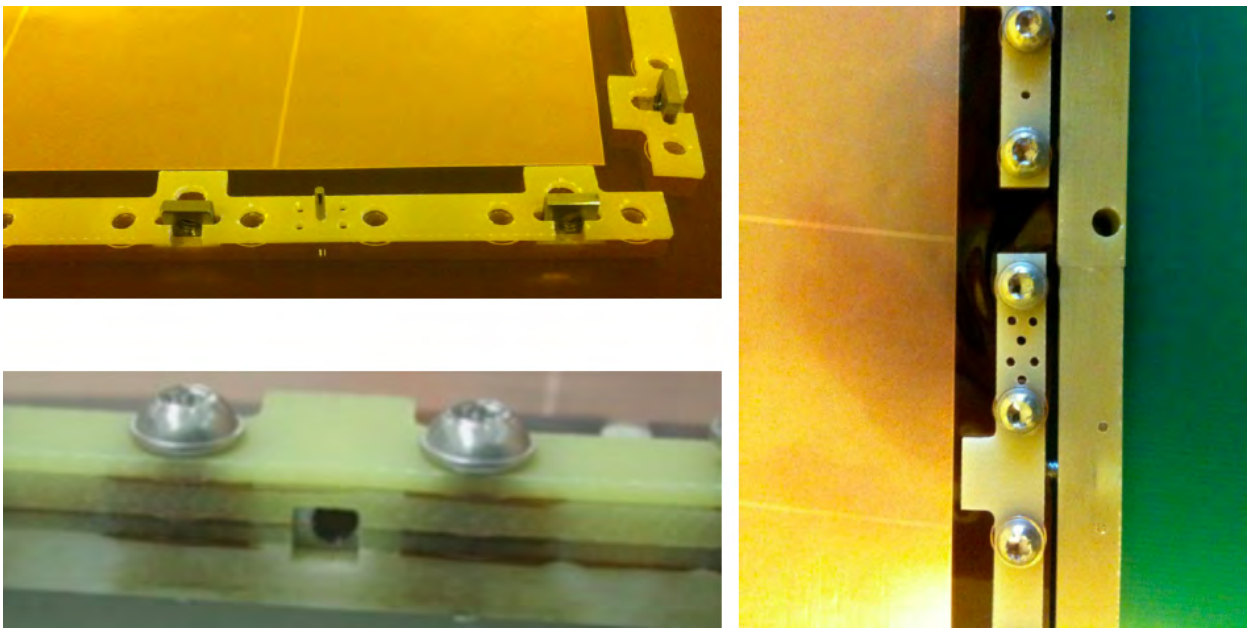

FIG. 7: Photographs of the CMS NS2 frames at CERN. Upper left: single layer of the inner frame showing a groove with an embedded nut to hold the stretching screw. Lower left: Bolted inner frame stack to clamb all layers, showing the hole with the embedded nut for the stretching screw. Right: Inner frame stack with horizontal screws through the outer frame for stretching. The gap between inner and outer frame is a few mm to accomodate the tension.

The GEM detectors constructed for the proposed experiment were based on the CMS design, but modified to minimize material in the active area. The inner stack consists of five layers, Drift, 3x GEM, and Readout, which are clamped together by inner frame parts (see Fig. 7). The inner frames contain embedded nuts in horizontal orientation that allow them to be bolted and stretched through a stiff outer frame, which is large enough to avoid any deformation. Figure 8 shows a schematic view of the double-frame structure with the clamped inner stack of the GEMs for DarkLight Phase 1c.

This structure is sandwiched between a top and bottom lid with thin chromium coated Kapton windows. The lid frames are bolted to the outer frame and O-ring sealed.

The setup guides the Readout layer past the sealed gas volume out to the exterior, in

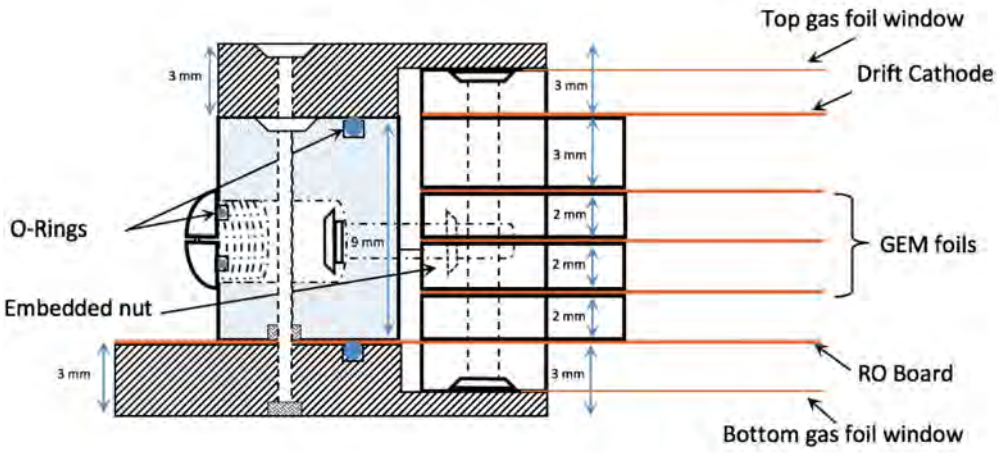

FIG. 8: Schematic view of the NS2 double frame mechanical system to provide simultaneous stretching of a clamped stack of foils.

order to interface with readout and to supply high voltage. Standard-CERN ceramic low-impedance passive voltage dividers are used. The individual voltages are guided through the inner frame stack to each respective layer, with spring-loaded pins, as indicated in Fig. 9. The GEM foils have been segmented into ten sectors, with an SMD resistor at the entrance to

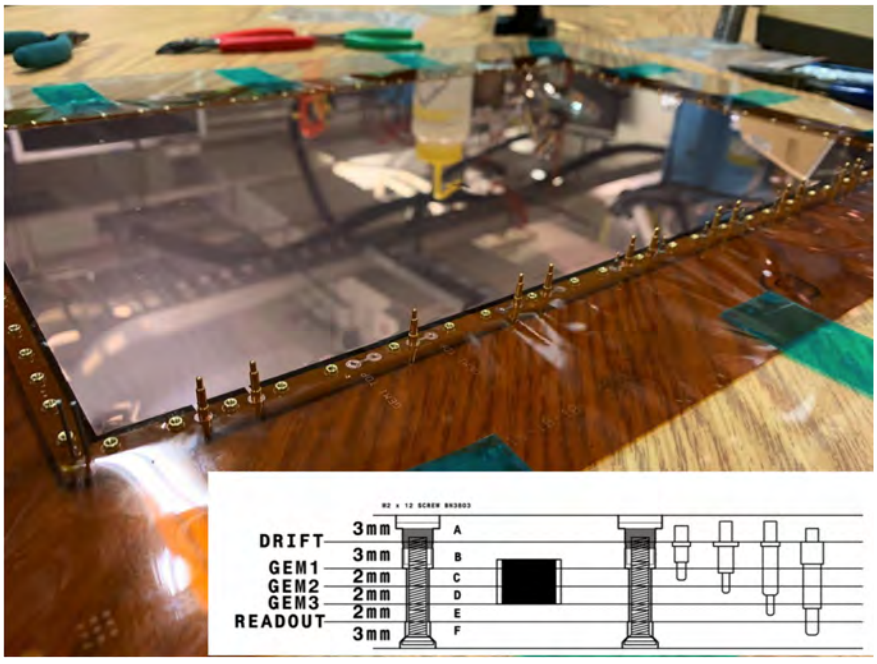

FIG. 9: Photo of the drift foil layer with spring loaded high-voltage pins to distribute the voltages picked up from the readout board to each GEM foil layer.

each pad for protection against shorts. Figure 10 shows photos of the realized GEM detector: of the inner frame stack before stretching (left), and with the main frame surrounding the inner stack and after stretching (right).

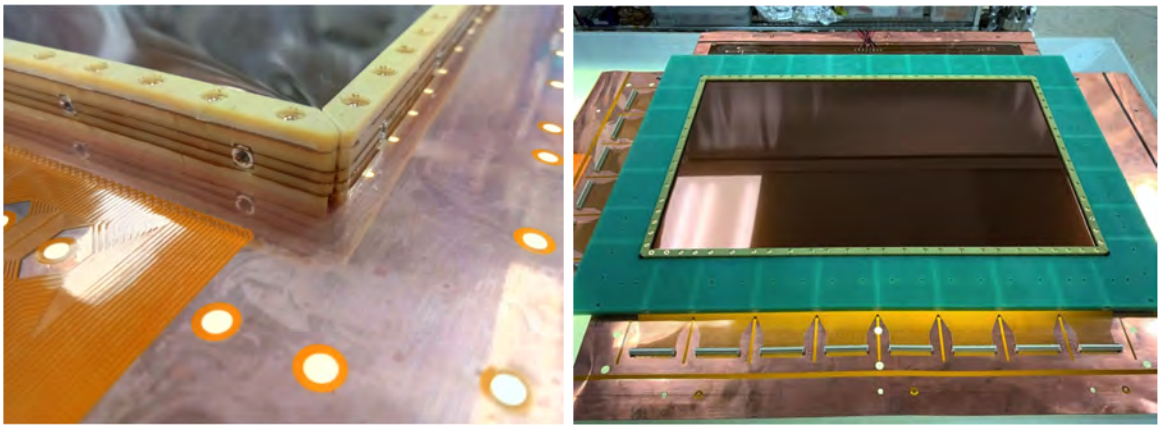

FIG. 10: Left: Inner frame stack after trimming excess foils and before stretching. The embedded nut for stretching can be seen. Right: View of the GEM detector after stretching with screws inserted through the rigid outer main frame.

Readout

The readout chain of the GEM setup is based on Analog Pipeline Voltage (APV) chips and Multi-Purpose Digitizers (MPDs), which were acquired for a total of eight chambers.

APV backplanes (Fig. 11) feed the operating low voltage to the APV chips and provide digital and analog connections to the MPD. One MPD can process up to 16 APVs in four groups of four. With the latest MPD firmware version 4 allowing fast VME modes as well as optical readout only up to 15 APVs can be connected. In the realized design, each GEM chamber (13 APVs) is read out with one MPD.

The fast VME readout mode was implemented in the DAQ software, the readout time for 13 APVs of one GEM was reduced from about 1 ms in BLT mode (32-bit block transfer) to now < 200 μs in 2eSST mode (64-bit block transfer).

Figure 12 shows a stack of two assembled GEM elements fully equipped with APV front-tend electronics, backplanes, analog and digital patch panels, and low-voltage regulator board.

Plan of Action

Eight GEMs were produced with funding from the DarkLight NSF MRI grant originally dedicated to DarkLight Phase-I. The NS2 scheme was implemented for the first time in a GEM detector optimized for low-energy nuclear physics.

After proposal PR12-18-006 had been deferred by PAC46, the HU group continued to

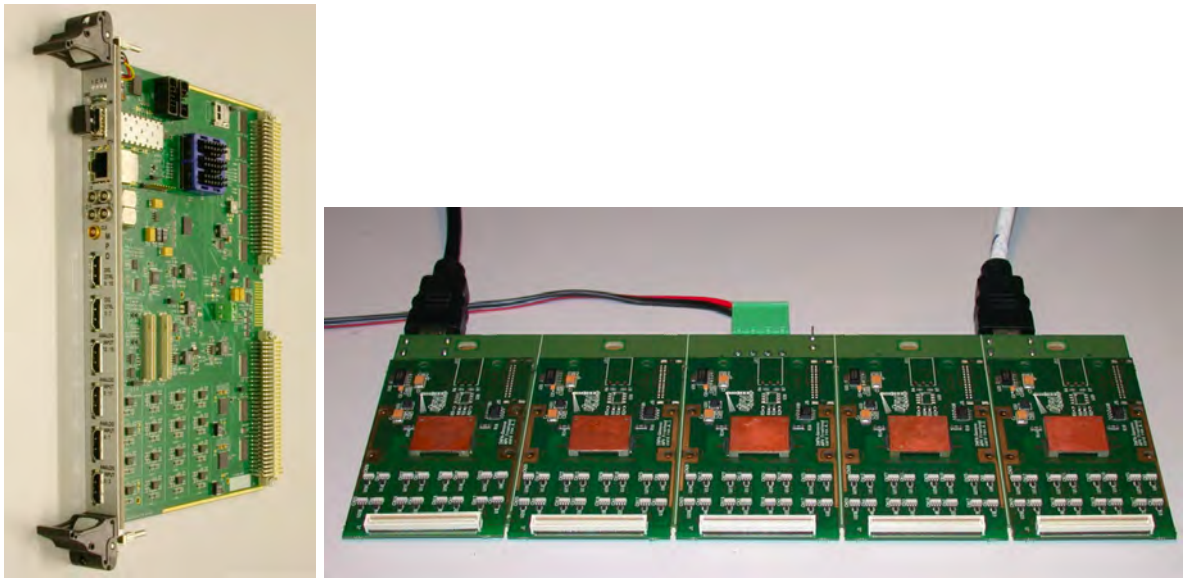

FIG. 11: Left: MPD4 VME module. Right: 5-slot APV backplane equipped with APV front-end v4.1.

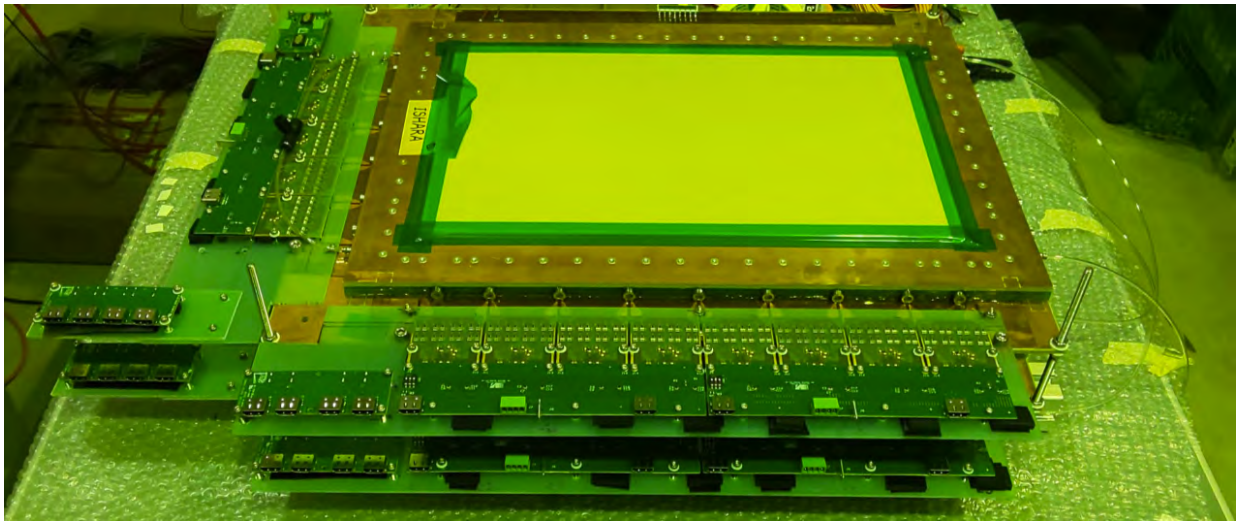

FIG. 12: Photo of two assembled GEM elements fully equipped with APV frontend electronics, backplanes, adapter boards and low-voltage regulator board.

TABLE III: The effect of spectrometer resolution on momentum resolution.

Measured quantity	Effect on invariant mass resolution
Relative momentum	$\frac{dM_A}{d\Delta p} = 85\,\mathrm{keV}/\%$
In-plane angle	$\frac{dM_A}{d\Delta\Theta} = 22\,\mathrm{keV}/mrad$
Out-of-plane angle	$\frac{dM_A}{d\Delta\Phi} = 5\ keV/mrad$

construct the GEM detectors, but at the same time developed plans to use these GEMs in other projects. Presently three GEM elements are situated at the Research Center for Electron Photon Science (ELPH) at Tohoku University in Sendai, Japan, where they are being commissioned for the ULQ2 program at ELPH. Another set of four elements has been planned to be added to the MUSE setup at PSI in Spring 2020, to augment the MUSE apparatus with tracking capability at forward angles. They are presently being commissioned at JLab with Sr-90 and cosmic rays. One more element is in production presently (as of December 2019). Unless these new commitments are canceled, it would be straightforward and require only modest funding to produce and test additional, identical GEM elements within 6-12 months. The required MPD and APV electronics are 100% compatible with those used at SBS and in PREX. Since operation of the proposed experiment and the SBS program in Hall A may likely not occur at the same time, no additional electronics are needed.

F. Count rates and reach

1. Signal

In the invariant mass spectrum of the detected particle pair, the signal process is essentially a delta function[2], so the observed width will be dominated by the detector resolution and energy loss processes. The effect of the detector resolution on the width of this peak is given in Table III. We believe the current spectrometer design can achieve a resolution of better than 150 keV. For the following discussion of reach, we use 250 keV as a conservative estimate.

[2]The width is $\Gamma \sim \alpha m_{A'} \epsilon_e^2$ which, in the region of the ^{8}Be anomaly, is sub-eV

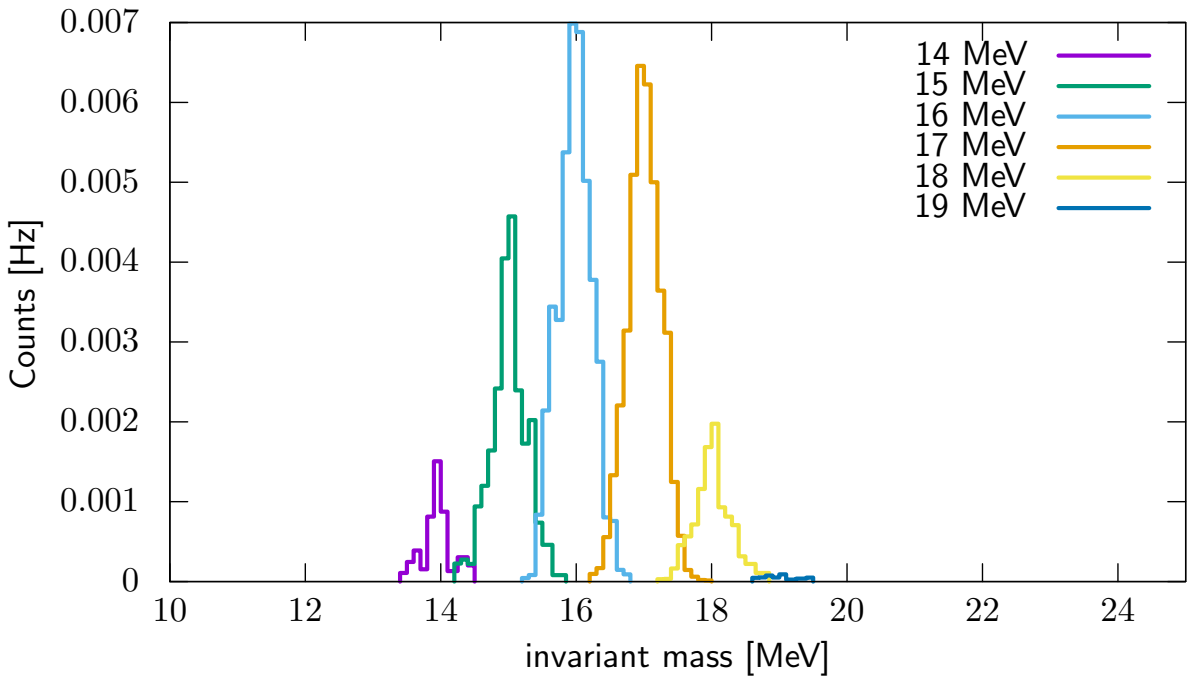

FIG. 13: Simulated signal and rates for A' candidates with a coupling of $\epsilon^2 = 10^{-6}$. Spectrometer acceptance was optimized for a 17 MeV mass, corresponding to the anomalous resonance in the ^{8}Be spectra.

The signal rate at design luminosity for multiple A' candidate masses at a benchmark coupling strength is shown in Figure 13.

2. Backgrounds

There are two main backgrounds, shown in Fig. 14: First, a lepton pair with an invariant mass of interest can be produced via initial or final state radiation of a Standard Model virtual photon, or via the trident graph. This is a physical irreducible background.

Secondly, the trigger condition can be fulfilled via random coincidences. A major source of these is the combination of a positron produced via SM pair production and an electron from elastic scattering, with internal bremsstrahlung reducing the electrons outgoing momentum to match the required momentum range.

Other sources of electrons of the required energy range include giant resonance electroproduction and quasielastic scattering, however the rates are substantially smaller.

Further sources of random coincidences are from beam-related room background. Ade-

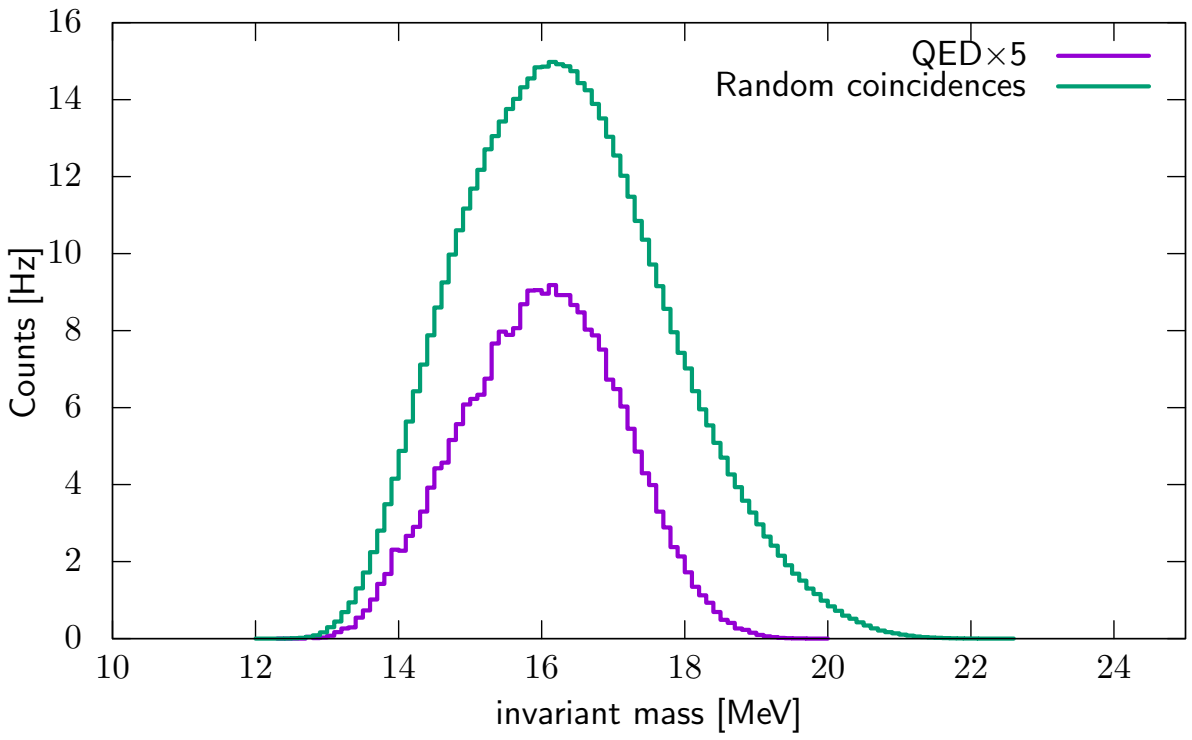

FIG. 14: Simulated background from QED diagrams and random coincidences.

quate shielding is required to reduce this to a tolerable level. Initial considerations indicate that such shielding is straight forward to implement in the hall.

The rate for random conincidences is give by the product of the individual rates, multiplied by the coincidence window. The smallest effective window is given by the bunch frequency, as it is not technically feasible to resolve times shorter than the bunch duration. For the CEBAF injector, the nominal bunch frequency is 1497 MHz, which results in an acceptable random trigger rate.

An overview of the rates are given in Table IV. As can be seen, for the proposed kinematics and beam conditions, the random coincidence background dominates. It is important to note that this background scales with $\mathcal{L}^2$. The figure of merit (FOM) is given by the number of signal events divided by the square root of the background events. Thus, for luminosities in which the accidental coincidence background dominates, the FOM is independent of $\mathcal{L}$ and only scales with the measurement time. In this sense, the proposed beam current and target thickness are optimal—a further increase in instantaneous luminosity would not yield a better reach. Figure 15 contains the Feynman graphs for the relevant signal and background processes.

V. LIMIT EXTRACTION

To extract a possible signal, an accurate description of the background is required. We note here that the dominant part of the background stems from random coincidences, which dominate the irreducible background by about a factor of 10. The random coincidence background can be extracted with excellent statistics via events recorded out of coincidence, and by event mixing, i.e. the combination of each event i in one detector which each event $j \neq i$ in the other. The QED background has to be simulated to extract the shape, however key simulation parameters can be cross checked by a simulation of the random coincidence background.

For Fig. 16 we simulate two random experimental outcomes, one with a signal at 17 MeV, one without. For each data set, we fit two models in a sliding window of 3 MeV width, one consisting of the irreducible background and random coincidence background, each with a fitted scaling parameter, and one with an additional Gaussian signal shape with fitted height but fixed width, centered in the fitted window. The p-value from an F-test as a function of the window position, as well as the extracted signal height is shown.

VI. EXPECTED REACH

We define our reach in terms of the region where a signal would have a 2σ significance compared to fluctuations of the standard model backgrounds. With 1000 hours (45 days) of

TABLE IV: Background rate estimates.

Type	Rate
QED irreducible background	coincidence: 55 Hz
	single e^+: 120 kHz
Elastic e-p with internal Brems.	single e^-: 6 MHz
Giant resonance electroproduction	200 kHz
Quasielastic electron scattering	160 kHz
Møller electron rate	0 (outside spectrometer acceptance)
Accidental coincidence rate	500 Hz

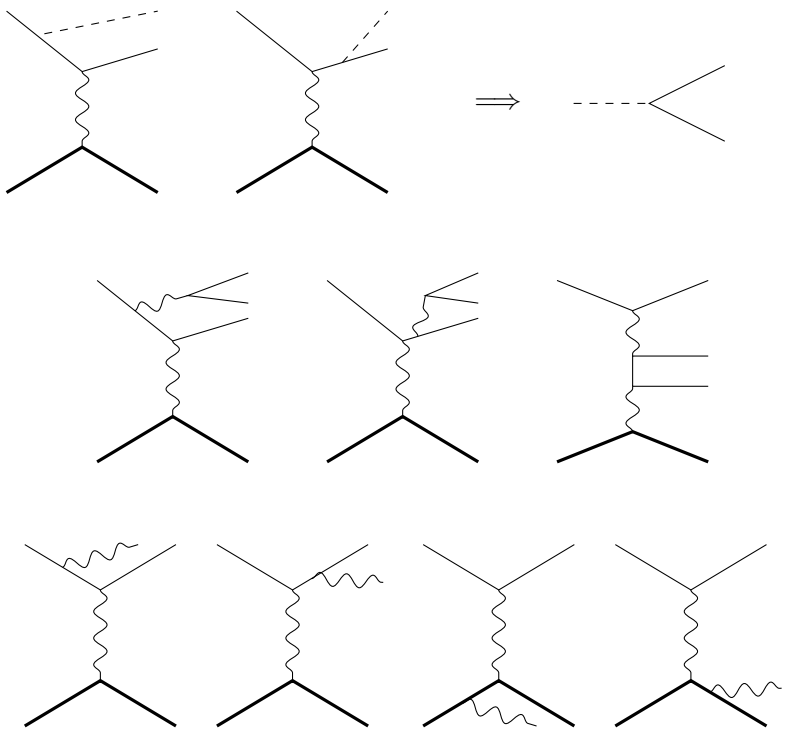

FIG. 15: Feynman graphs for the signal and dominant background processes. First row: The A' is produced off the incoming or outgoing lepton and then decays into an e^+e^- pair. The production off the proton legs is suppressed kinematically and additionally from the proto-phobic nature of the interaction. Second row: The irreducible QED background processes produce an e^+e^- pair via an intermediate virtual photon. Third row: The trigger condition can be fulfilled by accidental coincidences of an electron from radiative elastic scattering combined with a positron of the irreducible QED background. For the proposed kinematics and luminosity, this is the dominant background process.

running, the proposed experiment will probe all remaining untested coupling-mass parameter space of the ^{8}Be anomaly, including the overlap with the $g_\mu - 2$ anomaly region and down into the region excluded by NA64 [18]. We show this in figure 17 in the context of existing exclusions applicable to a proto-phobic force.

Future experiments which can probe the same region include Mu3e, with phase-1 data taking planned starting in 2021; an experiment at MESA, also planned to run post 2021, and an experiment at VEPP-3, currently only in it's planning phase. HPS will probe the parameter space in two modes, which are adjacent to, but do not overlap the region suggested

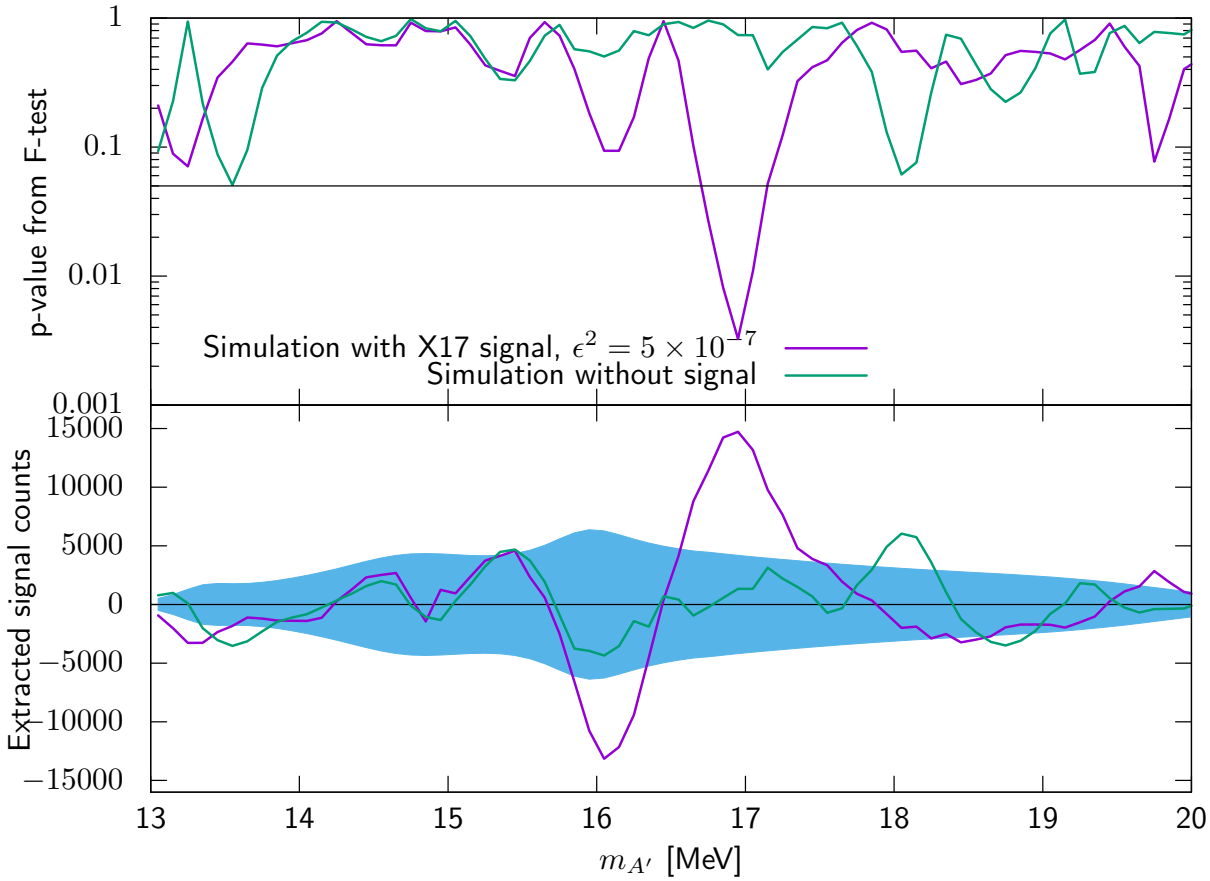

FIG. 16: Top: P-value for the null-hypothesis from an F-test for two simulated pseudo data sets. Bottom: Extracted signal strength for the two data sets. Blue shaded band is the one-sigma band for the extracted signal height. For the data set with a signal, the null-hypothesis is rejected, and a positive signal is found.

by the 5th force explanation. NA64 is in the R&D phase for a bump-hunt search which potentially could cover the whole area, but will not take data before the end of the long shutdown in 2021. The LHCb experiment will also be sensitive to this mass range in the dataset they intend to collect in LHC's Run 3, but due to the hadronic dependencies it is unclear what coupling strengths they will be able to probe.

VII. TEST PLATFORM FOR STREAMING READOUT

The proposed setup is ideally suited to be used as a streaming readout test system in a high-rate environment. While in principle, it is possible to retrofit the GEMs with a

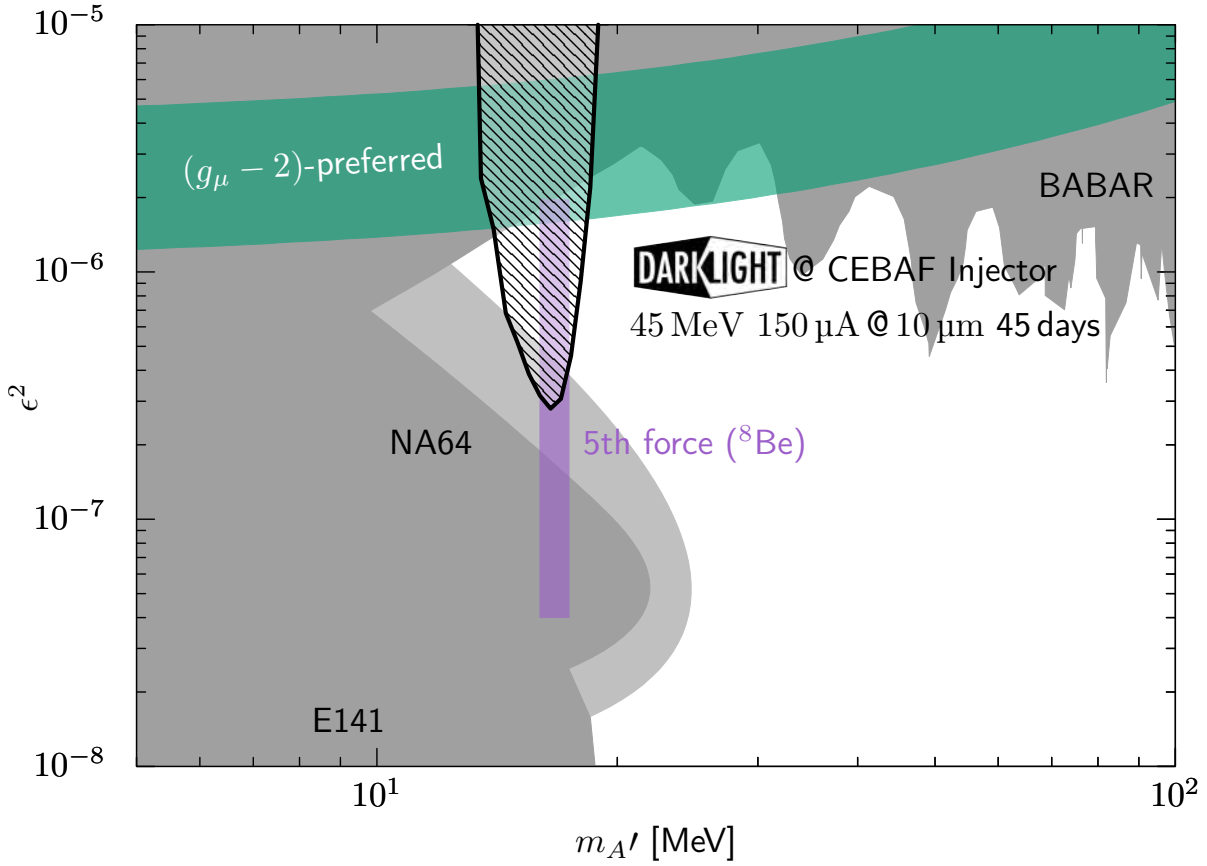

FIG. 17: Reach of the proposed experiment in comparison to existing exclusions (grey). The new exclusion limit from NA64 [18] is shown in light gray. With 1000 hours of delivered beam (45 days, assuming 100% duty factor), the experiment is sensitive to all of the as-yet unprobed portion of the proposed fifth-force parameter space.

streaming readout front end, the high channel count and requirement for ADC information makes this process comparatively pricey. On the other hand, the rather low resolution requirements in the focal plane make it possible to replace the GEM tracking detector with four layers of thin scintillator material, rotated 90 degrees to each other. This could be realized either in the form of scintillating fibers, or copying the design of the focal plane detector from the radiative Møller experiment.

For the latter, we tile the plane with 2.5 mm wide strips of 0.5 mm thickness, read out via SiPMs. The signal is then discriminated and read out with a TDC. A similar setup used at the MUSE experiment has proven to have time resolutions well below 100 ps.

Compared to ADC information from GEMs, where a reliable zero suppression has to take

the global, quickly varying baseline into account, the TDC information is sparse by nature. While standard, off-the-shelf TDC modules like CAEN's V1190 can be used in a streaming mode and could be used for a test setup, the full luminosity could not be handled. However, low cost, high resolution FPGA based solutions like TRB3 exist, as well as designs by the Jefferson Lab electronics group, which can handle these high rates.

A software defined trigger, or data selector, would then find coincidences between the two spectrometers. Since the full track information is available at this point, the timing can be corrected for path-length effect and the coincidence window can be very small. Since the DAQ is essentially dead-time free, a very efficient data taking is achievable.

VIII. REALIZATION

The major tasks involved in the proposed experiment are listed in Table V. The spectrometers will be designed and constructed at the MIT Bates R&E Center. The GEM detectors are being designed and constructed at Hampton University. The trigger hodoscopes will be built at MIT and Stony Brook University.

The necessary funds to construct the spectrometers, detectors and electronics were costed at about $130,000 in 2018, were requested from the DOE Office of Nuclear Physics in 2018 but subsequently withdrawn due to PAC46 action, and have been recently reviewed and revised to $150,000. Funding at Hampton University for the GEMS exists from the NSF Phase-1 MRI award. Once funding is available, it will take approximately 6-9 months to construct the experiment.

The DarkLight collaboration has six graduate students available to work on the proposed measurement: Sangbaek Lee, Patrick Moran and Robert Johnston from MIT; Malinga Rathnayake (M.S.) and Jesmin Nazeer (Ph.D.) from Hampton University, and Glenn Randall from Arizona State. In addition, it is expected that a student from Stony Brook University will join. They will work on the design, construction, commissioning and data taking phases of the experiment and write M.S. or Ph.D. theses on the results of the measurement. Jan C. Bernauer and Ross Corliss, both at Stony Brook University, are ready to take a leadership role in the proposed construction, installation and data taking portions of the experiment.

If the experiment is approved in early 2020 and funding is made immediately available, we expect to be ready to begin commissioning in summer 2020.

IX. BEAM TIME REQUEST

Subject to approval and funding availability, we propose to take data for 1000 hours (45 days) starting in 2020, at the CEBAF injector at a beam energy of 45 MeV with 150 µA current using the double spectrometer configuration and search in the e^+e^- invariant mass region of 17 MeV.

We additionally request 3 days for 1497 MHz accelerator commissioning and setup, and 7 days for the commissioning of the spectrometers. For this task, 4 K operation at 20 MeV is sufficient. It is best if these runs are scheduled in separate distinct periods.

TABLE V: Major tasks and responsibilities for the proposed experiment.

Task	Group	Description
Spectrometer magnets	MIT (led by Bates)	Preliminary design (complete)
		Optimization & detailed design (2018)
		Construction (Spring 2020)
		Field Mapping at JLab (2020)
GEM detectors	Hampton U.	Construction (2019)
		Assembly and testing (2020)
Trigger hodoscopes	MIT & Stony Brook	Optimization & detailed design (2020)
		Assembly and testing (2020)
Readout	MIT & Stony Brook	Slow controls & DAQ (2020)
Target	MIT	Detailed design (2020)
		Construction (2020)
Beam	JLab	Production, delivery,
		Diagnostics, tuning, beam dump
Analysis	MIT, Stony Brook	Carried out by the graduate students
	Hampton U.	

Appendix: The Low-Energy Møller Experiment at MIT

There has been renewed interest in Møller and Bhabha scattering as important signal, background, and luminosity-monitoring processes. The OLYMPUS experiment used these processes to monitor luminosity. For the DarkLight experiment, Møller scattering is the dominant scattering process in the forward direction. The Møller electrons are directed forward into a carefully designed dump (see Fig. 18), which was successfully tested in the August 2016 DarkLight commissioning run at the Jefferson Lab Low Energy Recirculator Facility (LERF).

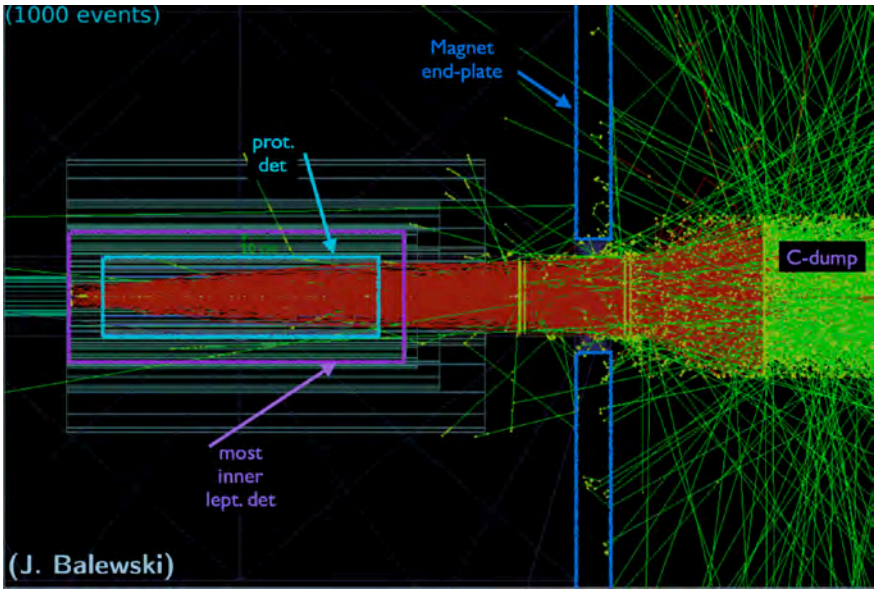

FIG. 18: Simulation of 1000 Møller scattered electrons (red lines) directed forward by the 0.5 T solenoidal field into the Møller dump. A large rate of photons (green lines) originating in the dump can cause significant background in the detector.

Møller scattered electrons may also radiate photons, a separate process, that, at the energies of interest, might be a significant additional background. To quantify this, we have carried out a calculation of the next-to-leading-order radiative corrections to unpolarized Møller and Bhabha scattering without resorting to ultra-relativistic approximations [19]. In this work, we have extended existing soft-photon radiative corrections with new hard-photon bremsstrahlung calculations so that the effect of photon emission is taken into account for any photon energy. This formulation was motivated by the needs of the OLYMPUS experiment and the upcoming DarkLight experiment, but is applicable to a broad range of experiments

at energies where QED is a sufficient description.

Radiative Møller scattering has not been measured to date, and it was one of the three scientific goals of the 2014 DarkLight NSF MRI award to measure the process at 100 MeV electron beam energy. After reevaluating the radiative Møller spectrum including the electron mass, we discovered a lack of data in the low-energy regions with which to compare our calculation. As a result, we planned to directly measure radiative Møller scattering in order to verify our work in this region where the electron mass is important. Concretely, we aim to measure the top 10% of the radiative Møller electron momentum spectrum at five different angles between 25° and 45°.

With the unavailability of the Jefferson Lab LERF for the foreseeable future, we completed a measurement of low-energy Møller scattering in summer 2018 at 2.5 MeV electron beam energy at the MIT High Voltage Research Laboratory (HVRL) [20]. Here, a Van de Graaff accelerator provided a monochromatic electron beam between 0.5 MeV and 3 MeV. This work formed the basis of the Ph.D. thesis of MIT graduate student Charles Epstein. The energy region is particularly interesting because it is precisely the region in which the electron mass is important, even more so than at 100 MeV. The HVRL beam energy is known to about ±20 keV. We have designed and constructed [21] a Faraday cup to provide a precise measurement of the beam current.

We note that, while the incoming beam energy drops by a factor of 40, the energy of the Møller scattered electrons drops by less than a factor of three. Fig. 19 shows the scattered non-radiative electron momentum as a function of angle, for selected beam energies between 1 and 100 MeV. Since the scattered electrons have similar energies, the same detector that was designed to run at the Jefferson Lab LERF will also work for a measurement at the HVRL. Fig. 20 shows the momentum spectrum at the HVRL at a scattering angle of 25° as calculated from [19].

The experimental apparatus consisted of a target chamber and a movable spectrometer arm, both mounted on a table to allow precision positioning and alignment. The spectrometer was designed and constructed at the MIT-Bates Research and Engineering Center. Both components were held under vacuum in order to minimize multiple scattering of the low-energy electrons.

The movable arm consisted of a 28 cm radius, 90°-bending dipole magnet, with a tungsten collimator at its entrance and a scintillating tile detector mounted on its focal plane. The

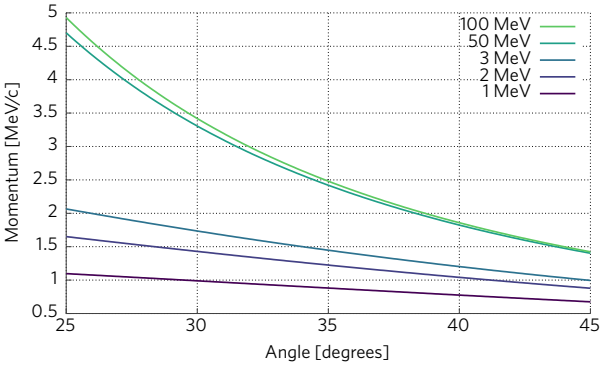

FIG. 19: Scattered Møller electron momentum as a function of angle for Møller scattering, for selected beam energies.

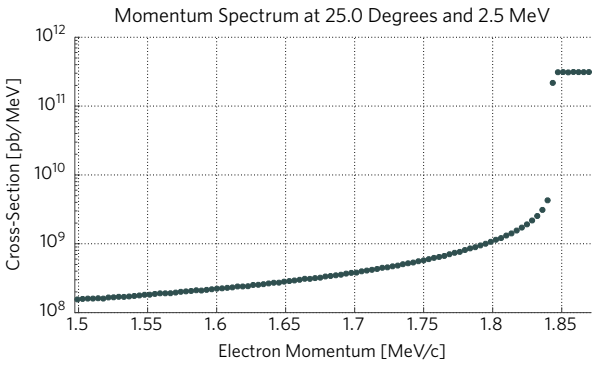

FIG. 20: Momentum spectrum from low-energy Møller scattering at a beam energy of 2.5 MeV at a scattering angle of 25° integrated over ±0.5°.

collimator defined a $1^\circ \times 1^\circ$ acceptance for electrons scattered from the target to enter the spectrometer; these electrons remained in vacuum until they passed through a Kapton window a few centimeters before the focal plane detector. The arm was constrained to move along a track, and locked into place at five positions between 25° and 45° with respect to the beam direction. Table VI summarizes the detector specifications.

TABLE VI: Detector specifications for the low-energy Møller experiment at the HVRL.

Dipole radius	28 cm
Dipole angle	90°
Distance of detector plane from target	60 cm
Momentum acceptance	$\Delta p/p \sim 10\%$
Momentum resolution	$\delta p/p \sim 10^{-3}$
θ acceptance	$\pm 0.5^\circ$
ϕ acceptance	1°
Møller signal angles	$25^\circ - 45^\circ$
Møller scattered electron momentum range	$0.9 - 2.1$ MeV/c
Spectrometer magnetic field range	100−350 Gauss

The target system was a remotely controllable ladder (re-using the mechanism from the

DarkLight 2012 beam test), on which were mounted various beam diagnostic elements as well as a set of diamond-like carbon foil targets with 1, 2, and 5-micron thicknesses, produced by MicroMatter [22].

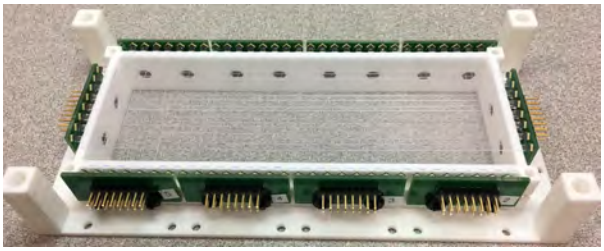

FIG. 21: The scintillating tile focal-plane detector, prior to being enclosed and installed.

The focal plane detector itself was a two-layer array of scintillating tiles instrumented with Silicon Photomultipliers (SiPMs). The tiles were 2.5 mm wide and 0.5 mm thick, arranged to cover an intended active area of 4 cm × 15 cm, corresponding to 16 tiles of 160 mm length (angle) and 60 tiles of 60 mm length (momentum). The tiles were made to our specifications by Eljen Technology and were diamond-milled in order to have optically-clear edges. The material was their EJ-212, which is based on a combination of polyvinyltoluene and fluors, and is similar to Saint-Gobain's BC-400.

The SiPMs were 2 mm Hamamatsu MPPC S13360-2050VE. These have a physical pitch of 2.4 mm and were built with TSV electrodes. To align with the 2.5 mm tiles, they were rotated by 45°. The tiles were read out alternately on the left and right sides, allowing the SiPMs to be spaced 5 mm apart rather than constricting them to 2.5 mm (Fig. 21). The MIT- designed amplifiers were intended to have single-photon sensitivity, high gain, and low noise. An on-board comparator enables digital LVDS output off the board to provide a TDC trigger.

The design was supported by a Geant4 simulation of the detector performance. Fig. 22 shows the simulated hit map on the focal plane detector for a 2.5 MeV beam at $25° \pm 0.5°$. Fig. 23 is a photograph of the experiment in 2018. Fig. 24 shows the measured yield [20] compared to a simulation based on the theoretical calculation [19].

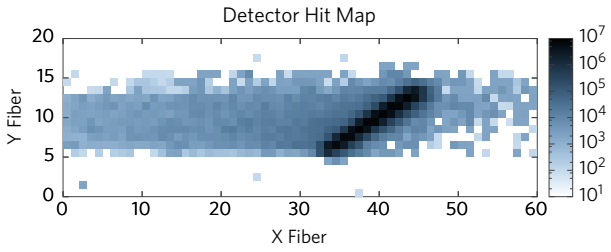

FIG. 22: Hit map on the focal plane detector for a 3 MeV beam at $25° \pm 0.5°$. *X Fiber* corresponds to momentum (lowest left), and *Y Fiber* scattering angle (lowest top).

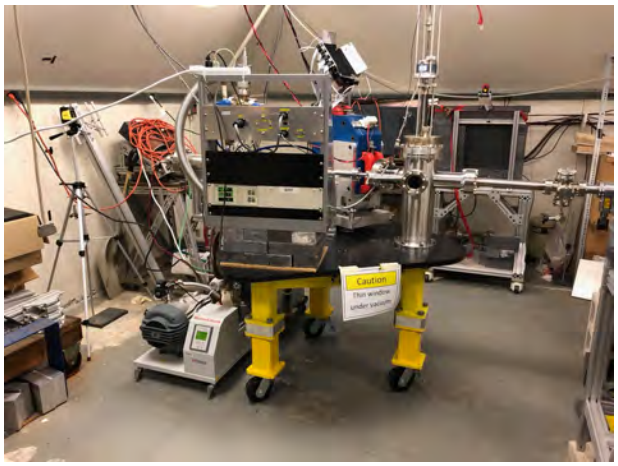

FIG. 23: The low-energy Møller experiment at the HVRL in 2018.

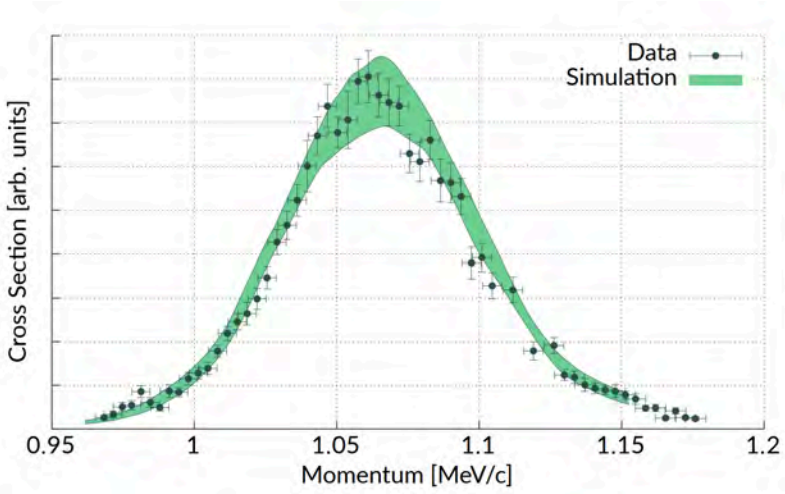

FIG. 24: Measured yield of scattered electrons vs. momentum compared to a simulation at an electron scattering angle of 40° from [20].

---

[1] F. Zwicky, Helvetica Physics Acta **6**, 110 (1933)

[2] R. Alarcon *et al.*, Phys. Rev. Lett. **111**, 164801 (2013).

[3] S. Lee *et al.*, Nucl. Instr. and Meth. A **939**, 46 (2019).

[4] C. Tschalär *et al.*, Nucl. Instr. and Meth. A **729**, 69 (2013).

[5] J.J. Aubert *et al.*, **33**, 1404 (1974).

[6] S. Abrahamyan *et al.*, Phys. Rev. Lett. **107**, 191804 (2011).

[7] R. Alarcon *et al.*, Nucl. Instr. and Meth. A **729**, 233 (2013).

[8] *Has a Hungarian physics lab found a fifth force of Nature?*, **Nature News**, 25 May 2016.

[9] *What scientists plan to do with the most powerful electron beam in the world*, **Washington Post**, June 25, 2016.

[10] *Dark matter - investigating the universe's hidden secrets*, **Research Features**, Issue #117, p.6, Research Publishing International Ltd., Westend, UK, November 2017.

[11] Richard G. Milner, *Understanding the Elusive Dark Matter*, Open Access Government, May 2018 see https://www.openaccessgovernment.org/understanding-the-elusive-dark-matter/44569/

[12] A. Krasznahorkay *et al.*, Phys. Rev. Lett. **116**, 042501 (2016).

[13] A. Krasznahorkay *et al.*, arXiv: 1910.10459, October 23, 2019.

[14] See https://www.cnn.com/2019/11/22/world/fifth-force-of-nature-scn-trnd/index.html https://www.independent.co.uk/news/science/dark-matter-particle-hungary-atomki-nuclear-research-force-nature-a9210741.html?amp

[15] X. Zhang and G.A. Miller, Phys. Lett. B**773**, 159 (2017).

[16] J. Feng *et al.*, Phys. Rev. Lett. **117**, 071803 (2016).

[17] D. Banerjee *et al.* [NA64 Collaboration], arXiv:1803.07748 [hep-ex].

[18] D. Banerjee *et al.* [NA64 Collaboratipn], arXiv:1912.11389 [hep-ex].

[19] Charles S. Epstein and Richard G. Milner, Phys. Rev. D **94**, 033004 (2016).

[20] Charles Epstein *et al.*, *Measurement of Møller Scattering at 2.5 MeV*, arXiv: 1903.09265, April 13, 2019, submitted to Phys. Rev. D.

[21] R. Johnston *et al.*, Nucl. Instr. and Meth. A **922**, 157 (2019).

[22] See: http://www.micromatter.com/dlc.php.